DECOUPLED DQ-CURRENT CONTROL OF GRID-TIED VOLTAGE SOURCE CONVERTERS

Aluru Venkata Siva Sainadh[1], Sravan Kumar.Dasari[2]
M.Venkateswara Reddy[3]

[1]*PG Student, Department of EEE, Vikas Group of Institutions, Nunna, Vijayawada, AP, (India)*
[2]*Associate Professor, Dept. of EEE, Vikas Group of Institutions, Nunna, Vijayawada, AP, (India)*
[3]*Associate Professor, Dept. of EEE, Vikas Group of Institutions, Nunna, Vijayawada, AP, (India)*

ABSTRACT

This paper presents an approach for the connection of a photovoltaic generator to the utility grid. A theoretical analysis, modeling, controlling and a simulation of a grid connected photovoltaic system using output LCL filters are described in detail. In order to reduce the complexity of the system, a linear voltage and current controllers have been developed for a three phase grid connected inverter. By this way, the inverter control system is simplified from third-order to first-order, and the close loop control system can easily be optimized for minimum steady-state error and current harmonic distortion. It utilizes the multi-input multi-output (MIMO) nonparametric model of the system along with a high-order linearly parameterized MIMO controller to form an open-loop transfer function matrix. Minimizing the second norm of the error between the open-loop transfer function matrix and a desired one, the coefficients of the controller are optimally determined. The characteristics of the inverter system with the proposed controller are investigated and compared with the traditional strategy.

Index Terms—Convex Optimization, Damping, High-Order Controller, LCL-Filter, Loop Shaping, Micro Grid, Resonance, Vector Control, Voltage-Source Converter (VSC)

I. INTRODUCTION

Renewable energy sources such as solar energy make increasing contributions to electric utility networks. Those sources are commonly coupled to the grid through a pulse width modulation inverter and filter [1]. Different output filter topologies are commonly used to interface inverter to the network, namely the L and the LCL filter. The use of the filter coupling the inverter to the grid reduces the high frequency pollution of the grid that can disturb loads [2]. They provide to the grid a nearly sinusoidal line current waveforms and a low line current distortion [3-5]. Of all filters used in the field of power electronic applications, the LCL filter is currently the most frequently used topologies [6]. Traditionally, L-filter is used as the interface between the grid network and the grid-connected voltage source inverters (VSI). With the L-filter, high switching frequency must be used to obtain high dynamic performance and sufficient attenuation of harmonics caused by the PWM. In contrast, the alternative LCL form of low-pass filter offers the potential for improved harmonic performance at lower switching frequencies, which is a significant advantage in higher-power applications [1], (e.g. fuel cell, wind generations). However, systems incorporating LCL filters are of third order, and they require more complex current control strategies to maintain system stability and are more susceptible to interference caused by grid voltage distortion because of resonance hazards and the lower harmonic impedance to the grid.

This paper proposes a vector control strategy for the LCL filter-based grid-connected VSCs that has inherent damping capability and does not require extra damping strategies. Moreover, the proposed vector control

strategy is able to fully decouple the dq-axes of the current. The design procedure shapes the open-loop and closed-loop transfer function matrices of the LCL-filter-based system. This is in contrast with the conventional approaches that design the controller matrix assuming an L-filter-based system. The proposed controller guarantees system stability and provides satisfactory and robust performance over a wide range of operating points. The elements of the controller matrix have an integrator similar to PI-controllers; however, they have more zeros, which permit the controller matrix to compensate for the potentially unstable poles of the LCL-filter-based system

II. STUDY SYSTEM DESCRIPTION

Fig. 1 shows the single-line diagram of the study system, which comprises a three-phase VSC interfaced to the utility grid though an LCL-filter and a coupling transformer. The filter is composed of a grid-side inductor Lg, a capacitor C, and a VSC-side inductor Lc. The internal resistance of Lg and Lc are represented by Rg and Rc, respectively. The VSC DC-side is fed by a continuous voltage source, and therefore, its dynamics are neglected in this paper. Table I presents the parameters of the study system of Fig. 1. According to the parameters of Table I, the resonance frequency of the LCL-filter-based system is calculated as follows:
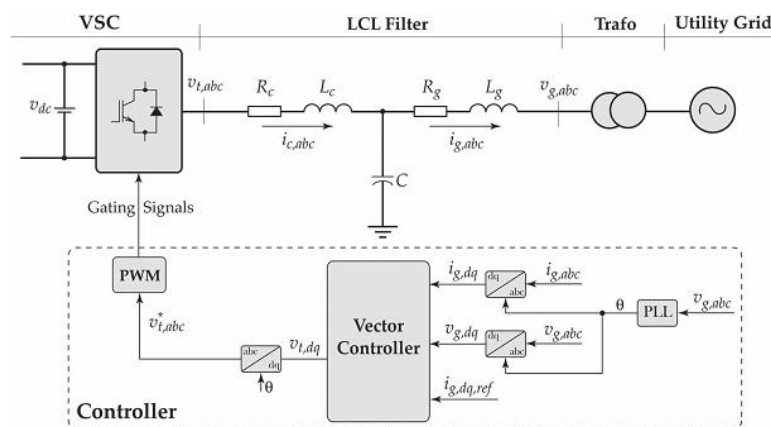

Fig. 1. Single-line diagram of the three-phase test system.

In the system of Fig. 1, for synchronization, a phase-locked loop (PLL) is utilized, which extracts the phase-angle of the grid voltage and forces its q-component to zero. Therefore, to regulate the real and reactive power exchange, a vector control strategy is adopted that controls the d- and q-components of the grid current, which are proportional to the real and reactive power, respectively. Feeding the errors between the dq-components of the grid current and their respective reference values to the controller, the control signals, i.e., the dq-components of the PWM block input signals, vt, dq, are then generated. The vector controller is also in charge of damping the system around its resonance frequency. All inputs/outputs of the proposed control system are illustrated in the respective block diagram of Fig. 1.

III. HIGH-ORDER DAMPING VECTOR CONTROL STRATEGY

In this section, the design procedure of the damping vector control strategy for LCL-filter-based VSCs is detailed, which is based on a constrained optimization-based loop shaping method. It uses the MIMO nonparametric model of the system, i.e., $G(j\omega)$, along with a linearly parameterized MIMO controller, i.e.,$K(z)$, to form an open-loop transfer function matrix, i.e.,$L(j\omega)=G(j\omega)K(j\omega)\forall\omega\in R$. Based on the dynamic performance

and the decoupling requirements, a desired open-loop transfer function matrix, i.e.,LD(s), is also formed, and its diagonal and off diagonal elements are determined. Minimizing the second norm of the error between the open-loop transfer function matrix and the desired one, the coefficients of the controller are optimally determined. To ensure the stability and the required dynamic performance of the closed-loop system, the minimization problem is subject to constraints. The design procedure is divided into three main steps: (1) the determination of the required nonparametric model, (2) the determination of the class of the controller, and (3) solving the optimization problem and finding the optimal coefficients of the controller. In the following, the steps are detailed.

A. Nonparametric Model

In order to design the damping vector control strategy, the first step is to determine the nonparametric model of the system. The goal of the vector control strategy is to regulate the dq-components of the grid current, i.e.,ig, dq, by providing the dq-components of the PWM input signals, i.e.,vt, dq. Therefore, the inputs of the to-be-controlled system are vt, dq, while its outputs are ig, dq. Thus, the system transfer function matrix is

$$\begin{bmatrix} i_{g,d} \\ i_{g,q} \end{bmatrix} = \underbrace{\begin{bmatrix} G_{11} & G_{12} \\ G_{21} & G_{22} \end{bmatrix}}_{\mathbf{G}} \begin{bmatrix} v_{t,d} \\ v_{t,q} \end{bmatrix}$$

(1)

To achieve the nonparametric model of the system of Fig. 1, exciting vt, d with a stimulus signal, e.g., pseudo random binary sequence (PRBS) , the frequency response ofG11andG21 could be identified as

$$G_{11}(j\omega) = \frac{\mathcal{F}(i_{g,d})}{\mathcal{F}(v_{t,d})} \quad \text{and} \quad G_{21}(j\omega) = \frac{\mathcal{F}(i_{g,q})}{\mathcal{F}(v_{t,d})}$$

(2)

The same holds for obtainingG22andG12through the excitation of vt, q. It must be noted that the identification sampling frequency, i.e., fs, id, could be different from the control sampling frequency, i.e., fs, and in this paper, fs, id=5kHz, which is compatible with the Shannon theorem. Fig. 2 depicts the identified nonparametric model corresponding to the system of Fig. 1, whose parameters are set according to Table I. The identified nonparametric model confirms
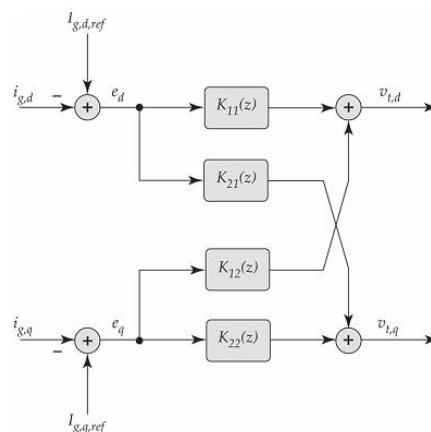

Fig. 2. Structural diagram of the controller.

the resonance phenomenon at frequencies around the predicted resonance frequency of 1677 Hz. Therefore, the controller matrix must be chosen and designed such that in the closed-loop system, the gains at frequencies around the resonance frequency are well attenuated.

B. Controller Class

The vector control strategy is responsible for regulating the dq-components of the grid current through manipulating the dq-components of VSC terminal voltage, i.e., vt, dq. Therefore, to control such a system, a 2 ×2 controller is required. A generic form of such a multivariable discrete-time controller in the z-domain is given by

$$\begin{bmatrix} v_{t,d} \\ v_{t,q} \end{bmatrix} = \underbrace{\begin{bmatrix} K_{11} & K_{12} \\ K_{21} & K_{22} \end{bmatrix}}_{\mathbf{K}} \begin{bmatrix} e_d \\ e_q \end{bmatrix}$$

(3)

Where d and eq are the current errors in the d- and q-axes, respectively. The structural diagram of the controller is depicted in Fig. 2. Conventional vector control strategies for L-filter-based VSCs utilize PI-controllers as the elements of the controller matrix [2], [3]. In such systems, only one dominant pole exists in each axis, which could be compensated by the zero of the utilized PI-controllers. In LCL-filter-based systems, however, this is no longer valid as more poles are introduced by the additional passive LC elements. Thus, if PI-controllers are used for the vector control of LCL-filter-based, all poles of the system may not be compensated, and therefore, damping strategies are required to attenuate the effects of the uncompensated poles. In this paper, high-order controllers are utilized as the elements of the controller in order to compensate for all poles of the LCL-filter-based system such that no extra damping strategies are required. Thus, each element of the controller matrix of (4) is a 5th-order controller in the z-domain. For example, K11is given by

$$K_{11}(z,\rho) = \frac{\rho_1 + \rho_2 z^{-1} + \rho_3 z^{-2} + \rho_4 z^{-3} + \rho_5 z^{-4} + \rho_6 z^{-5}}{1 - z^{-1}}$$

(4)

In which the vector ρ contains the controller matrix coefficients as follows:

$$\rho = [\rho_1, \rho_2, \ldots, \rho_{24}]$$

(5)

Therefore, the open-loop transfer function matrix of the LC L filter-based system is given by

$$\mathbf{L}(j\omega,\rho) = \mathbf{G}(j\omega)\mathbf{K}(j\omega,\rho) = \begin{bmatrix} L_{11} & L_{12} \\ L_{21} & L_{22} \end{bmatrix}$$

(6)

C. Optimization-Based Loop Shaping

The loop shaping of the open-loop transfer function matrix, i.e., L, is carried out by minimizing the square second norm of the error between the individual entries of Land a desired open-loop transfer function matrix, LD(s). Consequently, the control design procedure turns into an optimization problem as follows

$$\min_{\rho} \|\mathbf{L}(\rho) - \mathbf{L_D}\|^2$$

(7)

The desired open-loop transfer function matrix, LD, is chosen to meet the system requirements, e.g., satisfactory dynamic response and reduced coupling between the outputs, i.e., ig, d and ig, q. In this paper, the desired open-loop transfer function is selected as

$$\mathbf{L_D}(s) = \begin{bmatrix} \frac{\omega_c}{s} & 0 \\ 0 & \frac{\omega_c}{s} \end{bmatrix}$$

(8)

In which ωc= 1200rad/s. Note that the bandwidth of the closed-loop system is manipulated by the choice of ωc.
In order to ensure the stability and also the dynamic performance of the to-be-designed controller, the minimization problem is subject to several constraints. The reference proves that to shape the sensitivity function of the closed loop system, the minimization problem must be subject to the following linear constraints:

$$\left| W_1(j\omega) \left[1 + L_{Dq}(j\omega, \rho) \right] \right|$$
$$- \mathcal{R} \right] \left\{ \left[1 + L_{Dq}(-j\omega) \right] \left[1 + L_{qq}(j\omega, \rho) \right] \right\} < 0$$
$$\forall\, \omega \in \mathbb{R} \text{ and } q = 1, 2$$

(9)

whereW1 (jω) is a weighting filter. In this paper, W1 (jω) = 0.5, which guarantees a gain margin of at least 2 and a phase margin of greater than 29◦. Moreover, to ensure the stability of the closed-loop system, the minimization problem must satisfy the generalized Nyquist stability criterion. Therefore, as proved, the minimization problem must also satisfy the following constraints.
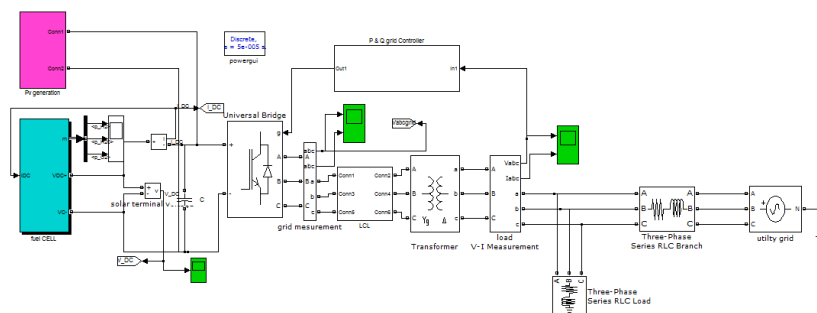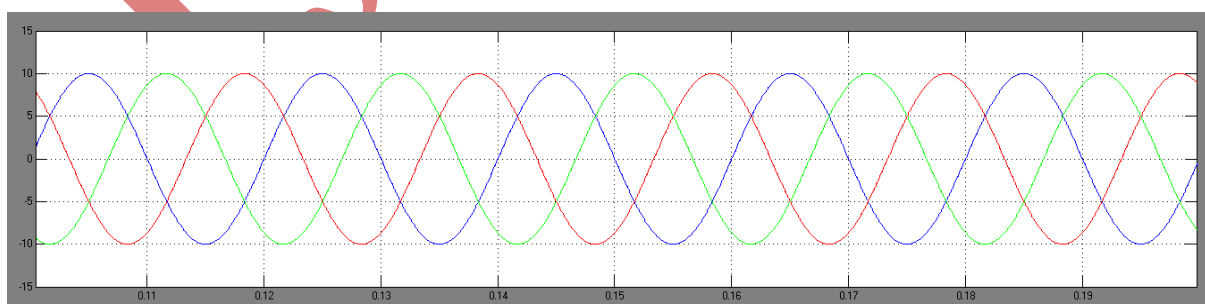
IV.MATLAB/SIMULINK RESULTS

Figure 3Matlab/Simulink High-Order damping vector control.

Figure 3shows the Matlab/Simulink High-Order damping vector control.
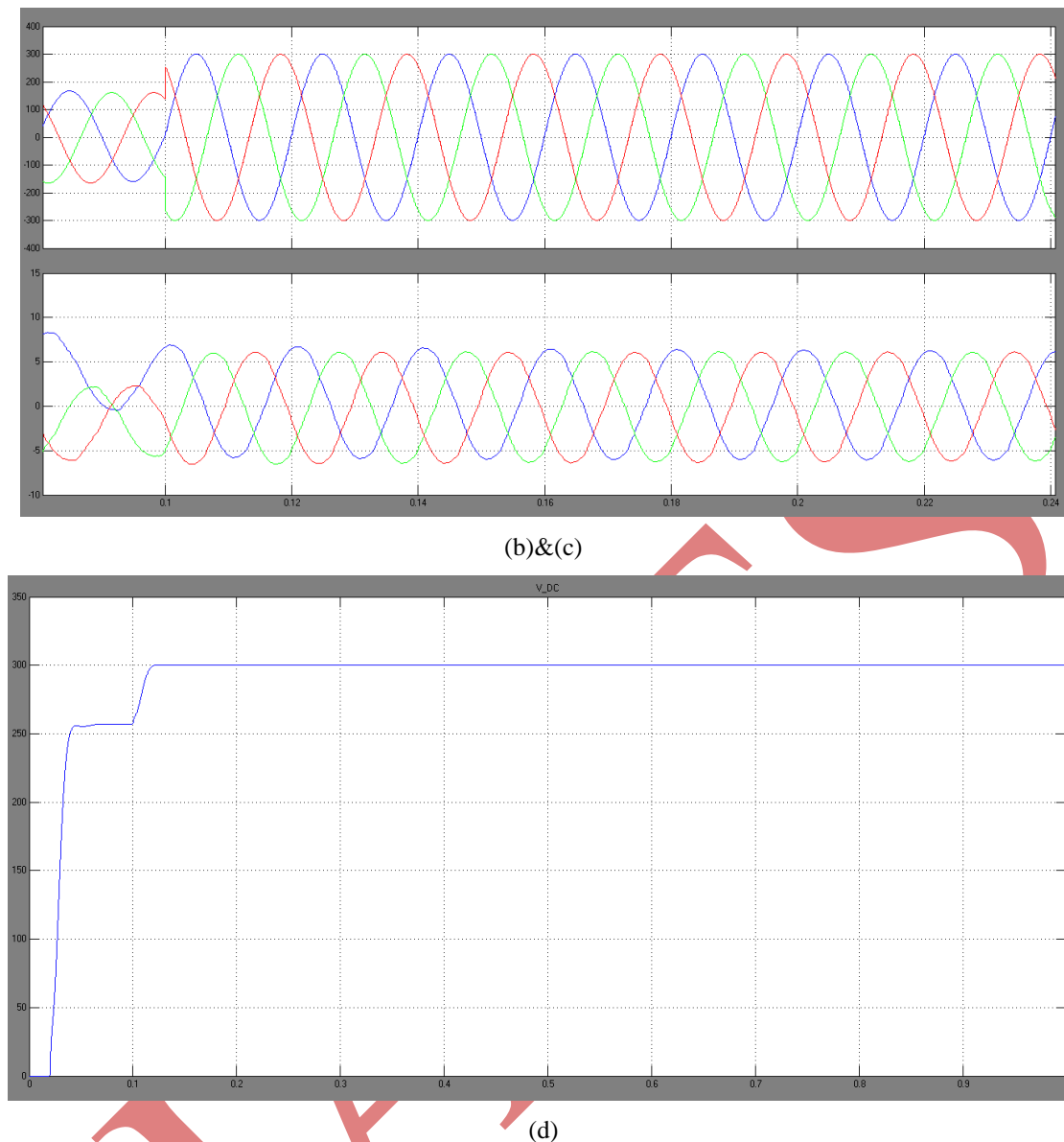

(a)

(b)&(c)

(d)

Fig.4. Simulation response of the system of the reference change in the d-axis while the LCL-filter parameters contain uncertainties: (a) the three-phase load voltage, (b) the three-phase grid current, (c) the three-phase converter current. (d) The d-and q-components of the grid current.

Reference Tracking in d-Axis: The reference value of the q-axis is kept constant at−6 A while the reference value of the d-axis steps up from−2 A to 5 A at the time instant t=20ms implying a change in the active power flow as well. Fig. 4(a) depicts the three-phase grid voltage, which remains unchanged during the reference tracking change. Fig. 4(b) and (c) show the three-phase converter and grid currents, respectively. The dq-components of the grid current, which are regulated by the high-order vector control strategy at their respective values, are also shown in Fig. 4(d). The latter confirms that upon the step-change in the d-axis, no resonance occurs in the system, and the reference value is tracked in almost 1 ms. Moreover, upon the step-change in the d-axis, the q-axis remains unchanged proving the decoupling capability of the proposed controller.

Subsequent to the step-change, the grid voltage experiences minor transients due to its internal impedance. In both aforementioned experimental tests, the three-phase grid and converter currents follow the requested

changes with zero steady-state error. Moreover, the currents do not contain resonance frequency ripples, which confirm the capability of the controller in terms of closed-loop system damping. In addition, it can be observed that in all cases, the experimental results are in very good agreement with the respective simulation results.
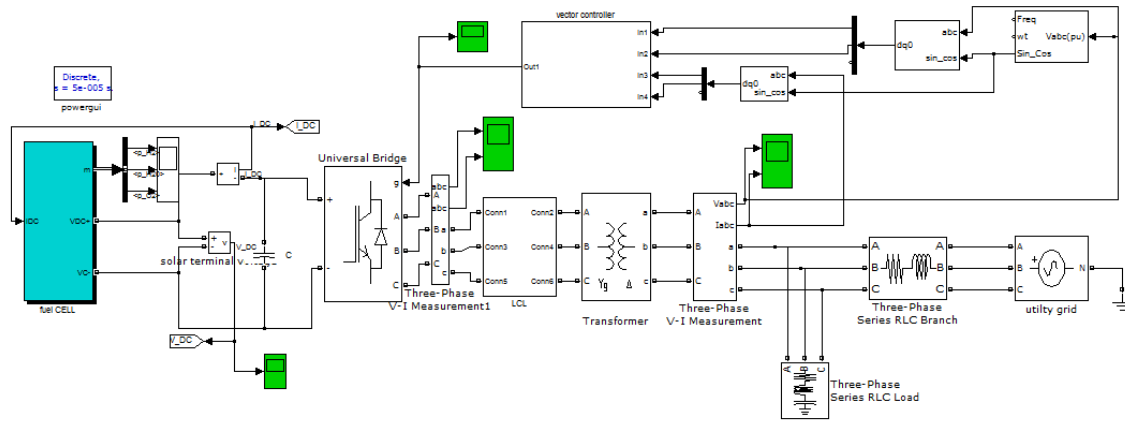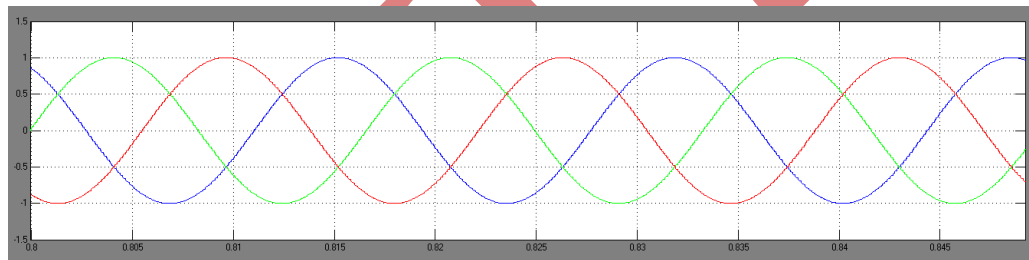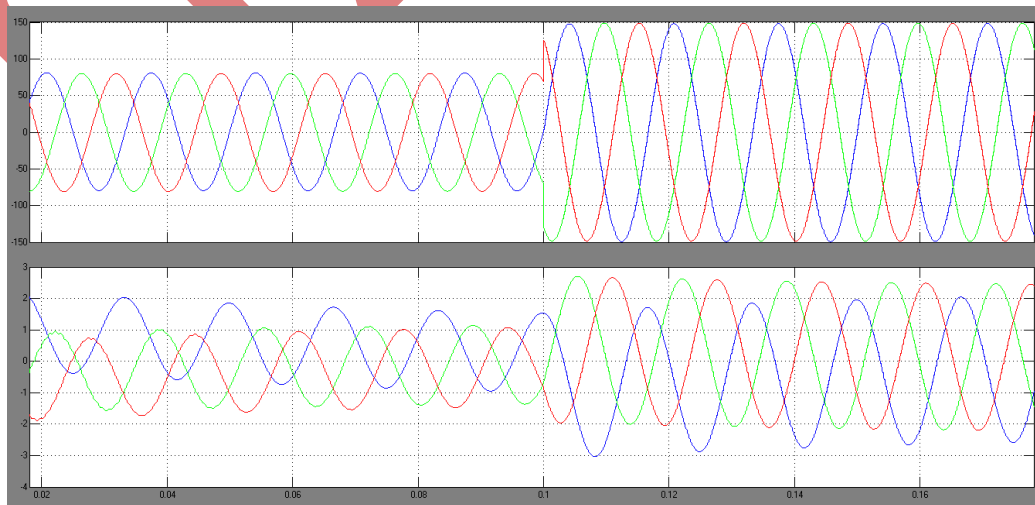

Figure5 Matlab/Simulink High-Order damping vector control with q-axis
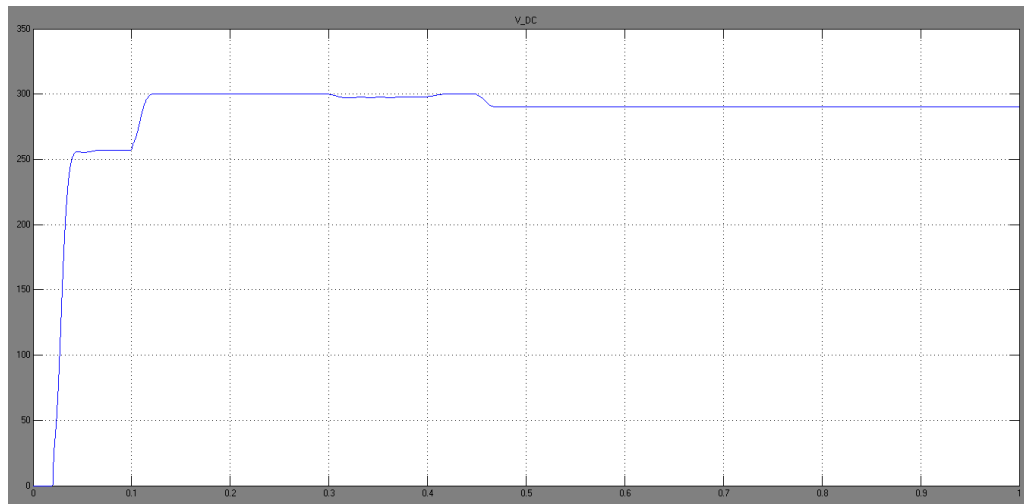
Figure5 shows the Matlab/Simulink High-Order damping vector control with q-axis

(a)

(b)&(c)

(d)

Fig.6. Simulation response of the system of the reference change in the q-axis while the LCL filter parameters contain uncertainties: (a) the three-phase grid voltage, (b) the three-phase grid current, (c) the three-phase converter current. (d) The d-and q-components of the grid current

Reference tracking in q-Axis: Another reference tracking test is carried out to evaluate the performance of the controller upon step-changes in the reference value of the q-axis while the reference value of thed-axisisfixedat6A. The reference value of the q-axis is stepped up from 0 to 8 A at the time instant t=20ms. Fig. 6(a)–(c) depict the three phase grid voltage, grid current, and converter current, respectively. Prior and subsequent to the step-change, the grid voltage remains unchanged, while the grid and converter currents are changed by the controller. Fig. 6(d) shows the dq-components of the grid current, which are regulated at their requested set-points. Upon the step-change in its reference value, the q-component reaches its final value in almost 1 ms, while the d-component is practically unaffected due to the decoupling effect of the controller. Moreover, the resonance is experienced neither upon the change of the reference signal nor in the steady-state operation.

V.CONCLUSION

A digital vector control strategy for the LCL-filter-based grid-connected VSCs is proposed in this paper. To damp the resonance phenomenon of the LCL-filter, a MIMO controller matrix is adopted, whose elements are linearly parameterized high-order controllers with integrators. Contrary to the existing vector control schemes for VSCs with LCL-filters, the proposed approach does not require extra damping methods. Moreover, the dynamic performance of the proposed approach is similar to the existing ones while its axis-decoupling capability is superior. The design procedure of the proposed controller is based on loop shaping and has three main steps: (1) attaining a nonparametric model of the system, (2) determining the class of the to-be-designed controller, and (3) solving a constrained convex optimization problem. Compared with the traditional strategies, the new control strategy has the superiority, and it is easy to be fulfilled. Thus, the new current control strategy is more attractive to grid-connected PV, fuel cell, and wind generation systems.

REFERENCES

[1] O. Senturk, L. Helle, S. Munk-Nielsen, P. Rodriguez, and R. Teodorescu, "Power capability investigation based on electro thermal models of press pack IGBT three-level NPC and ANPC VSCs for multi mega watt wind turbines," IEEE Trans. Power Electron., vol. 27, no. 7, pp. 3195–3206, Jul. 2012.

[2] B. Bahrani, A. Karimi, B. Rey, and A. Rufer, "Decoupled q-current control of grid-tied voltage source converters using nonparametric models," IEEE Trans. Ind. Electron., vol. 60, no. 4, pp. 1356–1366, Apr. 2013.

[3] B. Bahrani, S. Kenzelmann, and A. Rufer, "Multivariable-PI-based dq current control of voltage source converters with superior axis decoupling capability, "IEEE Trans. Ind. Electron., vol. 58, no. 7, pp. 3016–3026, Jul. 2011.

[4] B. Bahrani, A. Rufer, S. Kenzelmann, and L. Lopes, "Vector control of single-phase voltage-source converters based on fictive-axis emulation," IEEE Trans. Ind. Appl., vol. 47, no. 2, pp. 831–840, Mar./Apr. 2011.

[5] M. Liserre, R. Teodorescu, and F. Blaabjerg, "Stability of photovoltaic and wind turbine grid-connected inverters for a large set of grid impedance values," IEEE Trans. Power Electron., vol. 21, no. 1, pp. 263–272, Jan. 2006.

[6] P. Sun, C. Liu, J.-S. Lai, and C.-L. Chen, "Grid-tie control of cascade dual buck inverter with wide-range power flow capability for renewable energy applications, "IEEE Trans. Power Electron., vol. 27, no. 4, pp. 1839–1849, Apr. 2012.

[7] R. Teodorescu, M. Liserre, and P. Rodriguez,Grid Converters for Photovoltaic and Wind Power Systems. Hoboken, NJ, USA: Wiley, 2011.

[8] H. Akagi and R. Kondo, "A transformer less hybrid active filter using a three-level Pulse width Modulation (PWM) converter for a medium voltage motor drive," IEEE Trans. Power Electron., vol. 25, no. 6, pp. 1365–1374, Jun. 2010.

[9] V. Coroban-Schramel, I. Boldea, G.-D. And reescu, and F. Blaabjerg, "Active-flux-based motion-sensor less vector control of biaxial excitation generator/motor for automobiles, "IEEE Trans. Ind. Appl., vol. 47, no. 2, pp. 812–819, Mar./Apr. 2011.

[10] J. Chivite-Zabalza, M. Rodriguez Vidal, P. Izurza-Moreno, G. Calvo, and D. Madariaga, "A large power, low-switching-frequency voltage source converter for FACTS applications with low effects on the transmission line," IEEE Trans. Power Electron., vol. 27, no. 12, pp. 4868–4879, Dec. 2012.

[11] G. Kalcon, G. Adam, O. Anaya-Lara, S. Lo, and K. Uhlen, "Small-signal stability analysis of multi-terminal VSC-based DC transmission systems," IEEE Trans. Power Syst., vol. 27, no. 4, pp. 1818–1830, Nov. 2012.